



HAL
open science

Metamagnetic transition in the 75 K antiferromagnet $\text{Gd}_4\text{Co}_2\text{Mg}_3$

Stéphane Gorsse, Bernard Chevalier, Selcan Tuncel, Rainer Pöttgen

► **To cite this version:**

Stéphane Gorsse, Bernard Chevalier, Selcan Tuncel, Rainer Pöttgen. Metamagnetic transition in the 75 K antiferromagnet $\text{Gd}_4\text{Co}_2\text{Mg}_3$. *Journal of Solid State Chemistry*, 2009, 182 (4), pp.948-953. 10.1016/j.jssc.2009.01.027 . hal-00372463

HAL Id: hal-00372463

<https://hal.science/hal-00372463>

Submitted on 1 Apr 2009

HAL is a multi-disciplinary open access archive for the deposit and dissemination of scientific research documents, whether they are published or not. The documents may come from teaching and research institutions in France or abroad, or from public or private research centers.

L'archive ouverte pluridisciplinaire **HAL**, est destinée au dépôt et à la diffusion de documents scientifiques de niveau recherche, publiés ou non, émanant des établissements d'enseignement et de recherche français ou étrangers, des laboratoires publics ou privés.

Metamagnetic transition in the 75 K antiferromagnet $\text{Gd}_4\text{Co}_2\text{Mg}_3$

S. Gorsse ^a, B. Chevalier ^{a,*}, S. Tuncel ^b, R. Pöttgen ^b

^a *ICMCB, CNRS, Université de Bordeaux, 87 avenue du Docteur Albert*

Schweitzer, 33608 Pessac Cedex, France

^b *Institut für Anorganische und Analytische Chemie, Westfälische Wilhelms-*

Universität Münster, Corrensstraße 30, 48149 Münster, Germany

* Corresponding author. Tel.: +33 5 4000 6336; fax: +33 5 4000 2761. *E-mail*

address: chevalie@icmcb-bordeaux.cnrs.fr (B. Chevalier)

Abstract

$\text{Gd}_4\text{Co}_2\text{Mg}_3$ ($\text{Nd}_4\text{Co}_2\text{Mg}_3$ type; space group $P2/m$; $a = 754.0(4)$, $b = 374.1(1)$, $c = 822.5(3)$ pm and $\beta = 109.65(4)^\circ$) as unit cell parameters) was synthesized from the elements by induction melting in a sealed tantalum tube. Its investigation by electrical resistivity, magnetization and specific heat measurements reveals an antiferromagnetic ordering at $T_N = 75(1)$ K. Moreover, this ternary compound presents a metamagnetic transition at low critical magnetic field ($H_{\text{cr}} = 0.93(2)$ T at 6 K) and exhibits a magnetic moment of $6.3(1) \mu_B$ per Gd-atom at 6 K and $H = 4.6$ T. Due to this transition the compound shows a moderate magnetocaloric effect; at 77 K the maximum of the magnetic entropy change is $\Delta S_M = -10.3(2)$ J/kg K for a field change of 0-4.6 T. This effect is compared to that reported previously for compounds exhibiting a magnetic transition in the same temperature range.

Keywords: Gadolinium based compound; Magnetically ordered material; Metamagnet; Magnetocaloric effect

1. Introduction

The rare earth (*RE*)–transition metal (*T*)–magnesium systems have intensively been studied in the last ten years. Although more than 200 ternary compounds have been structurally characterized [1-6, and ref. therein] only little is known on their physical properties. Highly interesting compounds are the intermediate-valent systems $\text{Ce}_2\text{Ni}_2\text{Mg}$ and CeNi_4Mg [7], the metamagnet $\text{Pr}_2\text{Pd}_2\text{Mg}$ [8] presenting a low critical magnetic field, and the 43 K ferromagnet $\text{Nd}_2\text{Cu}_2\text{Mg}$ [9]. This last intermetallic exhibits a pronounced square loop behavior in its magnetization at 4.5 K.

Much higher magnetic ordering temperatures have been observed for the gadolinium based materials. Such compounds are of special interest with respect to their application potentials owing to a large magnetocaloric effect and giant magnetoresistance. For instance, $\text{Gd}_2\text{Ni}_2\text{Mg}$ shows antiferromagnetic ordering at 49 K [10], while stable ferromagnetic ground states have been observed for GdTMg ($T = \text{Pd, Ag, Pt}$) [11] with Curie temperatures of 95.7 K (GdPdMg), 39.3 K (GdAgMg), and 97.6 K (GdPtMg). Again, GdAuMg [12] orders antiferromagnetically at 81.1 K with a spin reorientation near 19 K. Several GdTMg intermetallics reveal slightly enhanced magnetic moments in the paramagnetic range, indicating a contribution of the gadolinium *5d* electrons induced via *4f-5d* exchange interactions.

During our systematic studies of the *RE-T-Mg* systems, we have started to investigate the gadolinium based compounds in more detail. Herein we report on

the electrical, magnetic and thermal properties of the gadolinium-rich phase $\text{Gd}_4\text{Co}_2\text{Mg}_3$ with crystallizes in the monoclinic $\text{Nd}_4\text{Co}_2\text{Mg}_3$ type structure [13, 14].

2. Experimental details

Starting materials for the synthesis of $\text{Gd}_4\text{Co}_2\text{Mg}_3$ were a gadolinium ingot (smart elements), cobalt powder (Sigma-Aldrich, 100 mesh, >99.9 %), and a magnesium rod (Johnson Matthey, \varnothing 16 mm, >99.95 %). The elements (4:2:3 atomic ratio) were arc-welded [15] in a small tantalum tube under an argon pressure of *ca.* 600 mbar. The argon was purified before over molecular sieves, silica gel and titanium sponge (900 K). The tantalum tube was placed in a water-cooled quartz sample chamber [16] of a high-frequency furnace (Hüttinger Elektronik, Freiburg, Typ TIG 1.5/300), first heated for 2 min at *ca.* 1300 K and subsequently annealed for 2 h at *ca.* 920 K, followed by quenching. The temperature was controlled through a Sensor Therm Metis MS09 pyrometer with an accuracy of ± 30 K. The brittle reaction product is stable in air over months.

The $\text{Gd}_4\text{Co}_2\text{Mg}_3$ sample was checked by X-ray powder diffraction (Guinier technique) using $\text{Cu K}\alpha_1$ radiation and α -quartz as an internal standard. The experimental pattern matched a calculated one [17] indicating pure $\text{Gd}_4\text{Co}_2\text{Mg}_3$ on the level of X-ray powder diffraction.

Magnetization measurements were performed using a superconducting quantum interference device (SQUID) magnetometer in the temperature range 4.2-300 K and applied fields up to 4.6 T. The measurement of the electrical

resistivity was carried out above 4.2 K on a bar of $1.5 \times 1.5 \times 5 \text{ mm}^3$ using a standard dc four probe method with silver paint contacts and an intensity current of 10 mA. Heat capacity measurement was realized by a relaxation method with a Quantum Design PPMS system and using a two τ model analysis.

3. Results and discussion

$\text{Gd}_4\text{Co}_2\text{Mg}_3$ [14] crystallizes with the monoclinic $\text{Nd}_4\text{Co}_2\text{Mg}_3$ type structure [13]. Since the crystal chemistry and the chemical bonding peculiarities were discussed in detail in previous work, we give only a brief account on $\text{Gd}_4\text{Co}_2\text{Mg}_3$ here. The coordination polyhedra of the two crystallographically independent Gd atoms (both with site symmetry m) are presented in Fig. 1. The Gd1 and Gd2 atoms have coordination numbers 16 and 14, respectively. Both Gd sites have closest Co neighbors with Gd–Co distances ranging from 272 to 294 pm, near to the sum of the covalent radii of 277 pm [18]. This is in line with recent electronic structure calculations [14] which revealed strong RE –Co interactions. Similar Gd–Co distances occur for the Gd_6 trigonal prismatic units in the other ternary compound rich in gadolinium Gd_4CoMg (281–282 pm) [19]. Both Gd sites have six nearest Gd neighbours 349–401 pm, similar to Gd_4CoMg (351–370 pm) [19]. These distances are comparable to *hcp* gadolinium (6×357 and 6×363 pm) [20].

The temperature dependence of the reduced electrical resistivity $\rho(T)/\rho(270 \text{ K})$ of $\text{Gd}_4\text{Co}_2\text{Mg}_3$ is shown in Fig. 2. (Owing to the presence of microcracks in the sample, absolute values of $\rho(T)$ could not be determined accurately; for this reason, we report the reduced resistivity). In the temperature range 280–77 K, the

resistivity exhibits metallic behaviour, decreasing almost linearly with the lowering of temperature. A sudden change of slope is detected at 77(1) K on the curve $\rho(T)/\rho(270 \text{ K})$ versus T , suggesting the occurrence of a transition which can be linked to the existence of an antiferromagnetic ordering as detected by magnetization measurement (see below). Finally, at low temperatures, below 23 K, $\rho(T)/\rho(270 \text{ K})$ data can be represented by a T^2 function (inset of Fig. 2) in reasonable agreement with the quadratic temperature dependence expected for a magnetic material.

The temperature dependence of the reciprocal magnetic susceptibility χ_m^{-1} of $\text{Gd}_4\text{Co}_2\text{Mg}_3$ in a magnetic field of $H = 3 \text{ T}$ is shown in Fig. 3(a) (inset). Above 120 K, the curve χ_m^{-1} versus T is fitted with a Curie-Weiss expression $\chi_m^{-1} = (T - \theta_p)/C_m$ where C_m is the molar Curie constant and θ_p the paramagnetic Curie temperature. The estimated effective moment $\mu_{\text{eff}} = (8C_m/n)^{1/2}$ (where $n = 4$ is the concentration of Gd^{3+} ions per mol) is found to be around 8.20(5) μ_B , which is slightly higher than the free-ion moment of the Gd^{3+} ion (7.94 μ_B). This suggests a contribution to the magnetic properties of $\text{Gd}_4\text{Co}_2\text{Mg}_3$ from (i) the cobalt atoms or/and (ii) the conduction electrons as observed previously for the intermetallics GdAgMg and GdPtMg [11]. Also, the positive value of $\theta_p = 83(1) \text{ K}$ indicates the predominance of the ferromagnetic interactions in this ternary compound.

For an applied magnetic field of $H = 0.025 \text{ T}$, the curve M/H versus T ($M =$ magnetization) exhibits a sharp maximum at about $T_N = 75(1) \text{ K}$ suggesting an antiferromagnetic ordering (Fig. 3(a)). This Néel temperature T_N agrees with that where the electrical resistivity presents a sudden decrease (Fig. 2). For higher

fields H , the maximum observed from the curves M/H versus T is both enlarged and shifted towards lower temperatures; for instance, for $H = 0.1$ and 0.2 T, the maximum appears at $72(1)$ and $63(1)$ K, respectively (Fig. 3(a)). This behaviour characterizes a metamagnetic transition occurring at very low critical magnetic fields as observed for the ternary stannide $\text{UCo}_{1.45}\text{Sn}_2$ [21]. This transition antiferromagnetic \rightarrow ferro(ferri)magnetic is confirmed by magnetization measurements at high magnetic fields. For $H = 0.85$ and 1 T (Fig. 3(b)), the curves M/H versus T exhibit: (i) a sharp increase in the magnetization at the Curie temperature $T_C = 81(1)$ K (this T_C -temperature was defined by the maximum appearing in the $\partial(M/H)/\partial T$ versus T derivative curves) and (ii) a small decrease of M below $12(1)$ K for $H = 0.85$ T but this behaviour is not observed for $H = 1$ T where M presents a saturation at low temperatures. These results indicate that the magnetic ordering of $\text{Gd}_4\text{Co}_2\text{Mg}_3$ is strongly dependent of the H -field.

The curves M versus H presented in Fig. 4 for various temperatures below T_N , confirm that $\text{Gd}_4\text{Co}_2\text{Mg}_3$ is a metamagnet. Clearly at $T = 6$ K, the magnetization, as H increases, varies linearly for $H < 0.2$ T (Fig. 4(a)) and then increases rapidly towards saturation (Fig. 4(b)). The metamagnetic transition occurs at lower magnetic fields as the temperature is increased; for instance at the Néel temperature ($T_N = 75(1)$ K), this transition is not detected. Moreover, isothermal magnetization performed at low temperatures, for instance at 6 K (Fig. 4(b)), saturates at $H = 4.6$ T with $25.2 \mu_B/\text{mol}$ or $6.3(1) \mu_B$ as saturation magnetic moment per Gd-atom, a value significantly smaller than the theoretically one calculated free Gd^{3+} -ion ($7 \mu_B$). This result suggests: (i) either a small

antiferromagnetic contribution of the cobalt atoms induced by the strong Gd-Co bonding [14] or (ii) that the metamagnetic transition evidenced for this ternary compound leads to a ferrimagnetic arrangement for the gadolinium substructure formed by two crystallographically independent Gd atoms.

Combining the results determined from the measurements M/H versus T and M versus H , we can draw a tentative magnetic phase diagram for $Gd_4Co_2Mg_3$ (Fig. 5). Three magnetic phases are distinguished: (i) the paramagnetic (P) phase; (ii) the antiferromagnetic (AF) phase observed at low magnetic fields and (iii) the ferro(ferri)magnetic (F) arrangement appearing after the metamagnetic transition. The borderline between the (AF) and (F) phases is deduced from the peak (in magnetic field) observed in the $\partial M/\partial H$ versus H derivative curves whereas that between (F) and (P) is determined from the maximum (in temperature) observed in the $\partial(M/H)/\partial T$ versus T derivative curves. We note that the critical magnetic field H_{cr} inducing the metamagnetic transition, varies practically linearly with the temperature; at 6 K, H_{cr} takes a small value of 0.93(2) T whereas at 1 T (Fig. 3(b)) the (AF) phase is not detected. This result indicates that the metamagnetic behaviour of the ternary compound $Gd_4Co_2Mg_3$ is easily observable in agreement with the positive value of the paramagnetic Curie temperature $\theta_p = 83(1)$ K.

Specific heat $C_{p,0}$ measured without applied magnetic field for $Gd_4Co_2Mg_3$ is shown in Fig. 6 as a function of temperature. The most important feature is the well defined λ -type anomaly signalling the antiferromagnetic transition. The ordering temperature is associated with the maximum at 75(1) K, in excellent agreement with that determined from magnetization and electrical resistivity

measurements. The tails above T_N suggest the existence of short range magnetic correlations.

The magnetic entropy change associated to the magnetic ordering of $\text{Gd}_4\text{Co}_2\text{Mg}_3$, ΔS_M , is calculated for both observed transitions from the isothermal magnetization M versus H curves using the well-known Maxwell relationship [22]:

$$\Delta S_M = \int_0^H \left[\frac{\partial M}{\partial T} \right] dH. \quad (1)$$

The sign of ΔS_M is positive for the (F) to (AF) metamagnetic transition and negative for the (P) to (F) ordering transition (Fig. 7). The ternary compound $\text{Gd}_4\text{Co}_2\text{Mg}_3$ exhibits both a magnetocaloric effect (MCE) at 77 K giving rise to a temperature increase when applying a magnetic field adiabatically and an inverse MCE at 6 K that cools the sample.

The inverse MCE gives rise to a moderate entropy increase of $0.56(2) \text{ Jkg}^{-1}\text{K}^{-1}$ at 6 K under the application of field of 1 T. In $\text{Gd}_4\text{Co}_2\text{Mg}_3$, inverse MCE resulting of the (F) to (AF) transition can be attributed to the presence of two different crystallographic sites for Gd atoms and different Gd-Gd interatomic distances.

The peak entropy change at 77 K in a magnetic field of 2 and 4.6 T reaches $-5.8(2)$ and $-10.3(2) \text{ Jkg}^{-1}\text{K}^{-1}$, respectively. These values are comparable to that observed for the metamagnet Gd_3Co ($\Delta S_M = -11 \text{ Jkg}^{-1}\text{K}^{-1}$ near 140 K and $H = 5 \text{ T}$) [23] suggest that $\text{Gd}_4\text{Co}_2\text{Mg}_3$ could be useful for magnetic refrigeration around 77 K. The resulting refrigeration capacity, $\text{RCP} = \Delta S_{M,P \rightarrow F}^{\text{PEAK}} \cdot \delta T_{FWHM}$, is $500(10) \text{ Jkg}^{-1}$ for $\Delta H = 4.6 \text{ T}$ (δT_{FWHM} is the full width at half length of ΔS_M). Fig. 8 shows the

normalized $RCP/\Delta H$ plotted against the magnetic ordering temperature T_t for several compounds of references and high MCE Gd-based materials from the literature together with the $Gd_4Co_2Mg_3$ from this work. It can be seen that $Gd_4Co_2Mg_3$ exhibit the highest refrigeration capacity for working temperature in the range of 60-100 K.

The adiabatic temperature change, ΔT_{ad} , linked to the MCE can be evaluated using the relationship [24, 25]:

$$\Delta T_{ad}(T; 0 \rightarrow H) = -T\Delta S_M / C_{P,0}(T)$$

where $C_{P,0}(T)$ represents the specific heat measured without applied magnetic field. ΔT_{ad} reaches 1.3(1) and 3.4(1) K for $\Delta H = 2$ and 4.6 T, respectively.

Fig. 9 compares the normalized adiabatic temperature change, $\Delta T_{ad}/\Delta H$, for $Gd_4Co_2Mg_3$ and other materials having the largest MCE between 10 and 80 K. In this temperature range, the application of magnetocaloric cooling is gas liquefaction. The $Gd_4Co_2Mg_3$ ternary compound from the present work competes well with these high-MCE intermetallic compounds bearing lanthanide metals.

4. Conclusion

$Gd_4Co_2Mg_3$ orders antiferromagnetically below $T_N = 75$ K and shows a field-induced transition at approximately 0.93 T at 6 K. This metamagnetic transition is closely associated with the fact that the paramagnetic Curie temperature is positive ($\theta_p = 83$ K). This means that the overall interaction between the Gd moments in this ternary compound is ferro(ferri)magnetic and that the antiferromagnetic ground state is rather unstable. We found a maximum value of

the magnetic entropy change ΔS_M of about $-10.3 \text{ Jkg}^{-1}\text{K}^{-1}$ at 77 K and a field change of 4.6 T, due to the field-induced magnetic phase transition. This value is comparable to that observed for the metamagnet Gd_3Co ($\Delta S_M = -11 \text{ Jkg}^{-1}\text{K}^{-1}$ near 140 K and $H = 5 \text{ T}$) [23] and suggests that $\text{Gd}_4\text{Co}_2\text{Mg}_3$ could be useful for magnetic refrigeration around 77 K.

Acknowledgments

This work was financially supported by the Deutsche Forschungsgemeinschaft. B.C. and R.P. are indebted to EGIDE and DAAD for research grants within the PROCOPE programs (11457RD and D/0502176).

References

- [1] U. Ch. Rodewald, B. Chevalier, R. Pöttgen, *J. Solid State Chem.* 180 (2007) 1720-1736.
- [2] U. Ch. Rodewald, S. Tuncel, B. Chevalier, R. Pöttgen, *Z. Anorg. Allg. Chem.* 634 (2008) 1011-1016.
- [3] J.-N. Chotard, Y. Filinchuk, B. Revaz, K. Yvon, *Angew. Chem. Int. Ed.* 45 (2006) 7770-7773.
- [4] G. Renaudin, L. Guénée, K. Yvon, *J. Alloys Compd.* 350 (2003) 145-150.
- [5] P. Solokha, S. De Negri, V. Pavlyuk, A. Saccone, B. Marciniak, *J. Solid State Chem.* 180 (2007) 3066-3075.

- [6] S. De Negri, A. Saccone, P. Rogl, G. Giester, *Intermetallics* 16 (2008) 1285-1291.
- [7] C. Geibel, U. Klinger, M. Weiden, B. Buschinger, F. Steglich, *Physica B* 237-238 (1997) 202-204.
- [8] R. Kraft, Th. Fickenscher, G. Kotzyba, R.-D. Hoffmann, R. Pöttgen, *Intermetallics* 11 (2003) 111-118.
- [9] G. Kotzyba, R. Mishra, R. Pöttgen, *Z. Naturforsch.* 58b (2003) 497-500.
- [10] K. Łątka, R. Kmieć, A. W. Pacyna, R. Mishra, R. Pöttgen, *Solid State Sci.* 3 (2001) 545-558.
- [11] K. Łątka, R. Kmieć, A. W. Pacyna, T. Tomkowicz, R. Mishra, T. Fickenscher, H. Piotrowski, R.-D. Hoffmann, R. Pöttgen, *J. Solid State Chem.* 168 (2002) 331-342.
- [12] K. Łątka, R. Kmieć, A. W. Pacyna, Th. Fickenscher, R.-D. Hoffmann, R. Pöttgen, *Solid State Sci.* 6 (2004) 301-309.
- [13] S. Tuncel, R.-D. Hoffmann, B. Heying, B. Chevalier, R. Pöttgen, *Z. Anorg. Allg. Chem.* 632 (2006) 2017-2020.
- [14] S. Tuncel, U. Ch. Rodewald, S. F. Matar, B. Chevalier, R. Pöttgen, *Z. Naturforsch.* 62b (2007) 162-168.
- [15] R. Pöttgen, Th. Gulden, A. Simon, *GIT Labor Fachzeitschrift* 43 (1999) 133-136.
- [16] D. Kußmann, R.-D. Hoffmann, R. Pöttgen, *Z. Anorg. Allg. Chem.* 624 (1998) 1727-1735.
- [17] K. Yvon, W. Jeitschko, E. Parthé, *J. Appl. Crystallogr.* 10 (1977) 73-74.

- [18] J. Emsley, *The Elements*, Clarendon Press, Oxford (1989).
- [19] S. Tuncel, R.-D. Hoffmann, B. Chevalier, S. F. Matar, R. Pöttgen, *Z. Anorg. Allg. Chem.* 633 (2007) 151-157.
- [20] J. Donohue, *The Structures of the Elements*, Wiley, New York (1974).
- [21] F. Mirambet, B. Chevalier, P. Gravereau, and J. Etourneau, *Solid State Commun.* 82 (1992) 25-28.
- [22] A. H. Morrish, *The Physical Principles of Magnetism*, Wiley, New York, 1964 (Chap. 3).
- [23] S. K. Tripathy, K. G. Suresh, A. K. Nigam, *J. Magn. Magn. Mater.* 306 (2006) 24-29.
- [24] V. K. Pecharsky, and K. A. Gschneidner Jr, *J. Magn. Magn. Mater.* 200 (1999) 44-56.
- [25] V. K. Pecharsky, K. A. Gschneidner Jr, A. O. Pecharsky, and A. M. Tishin, *Phys. Rev. B* 64 (2001) 144406.
- [26] A. M. Tishin, *J. Magn. Magn. Mater.* 316 (2007) 351-357.
- [27] S. Yu. Dan'kov, A. M. Tishin, V. K. Pecharsky, K. A. Gscheidner, Jr., *Phys. Rev. B* 57 (1998) 3478-3490.
- [28] S. A. Nikitin, A. M. Tishin, P. I. Leontiev, *J. Magn. Magn. Mater.* 92 (1991) 405-416.
- [29] S. Gorsse, B. Chevalier, G. Orveillon, *Appl. Phys. Lett.* 92 (2008) 122501-3.
- [30] S. Tencé, S. Gorsse, E. Gaudin, B. Chevalier, *Intermetallics* (2008)
doi:10.1016/j.intermet.2008.10.004

- [31] T. Hashimoto, K. Matsumoto, T. Kurihara, T. Numuzawa, A. Tomokiyo, H. Yayama, T. Goto, S. Todo, M. Sahashi, *Adv. Cryog. Eng.* 32 (1986) 279.
- [32] T. Hashimoto, T. Kuzuhara, K. Matsumoto, M. Sahashi, K. Inomata, A. Tomokiyo, H. Yayama, *Jpn. J. Appl. Phys.* 26 (1987) 1673-1674.
- [33] T. Hashimoto, T. Kuzuhara, M. Sahashi, K. Inomata, A. Tomokiyo, H. Yayama, *J. Appl. Phys.* 62 (1987) 3873-3878.
- [34] H. Takeya, V. K. Pecharsky, K. A. Gschneidner Jr., J. O. Moorman, *Appl. Phys. Lett.* 64 (1994) 2739-2741.
- [35] K. A. Gschneidner Jr., H. Takeya, J. O. Moorman, V. K. Pecharsky, S. K. Malik, C. B. Zimm, *Adv. Cryog. Eng.* 39 (1994) 1457.
- [36] J. A. Barclay, W. C. Overton Jr., C. B. Zimm, in: U. Ekren, A. Schmid, W. Weber, H. Wuhl (Eds.), *LT-17 Contributed Papers*, Elsevier Science, Amsterdam, 1984, p. 157.
- [37] C. B. Zimm, E. M. Ludeman, M. C. Severson, T. A. Henning, *Adv. Cryog. Eng.* 37B (1992) 883.
- [38] A. Tomokiyo, H. Yayama, H. Wakabayashi, T. Kuzuhara, T. Hashimoto, M. Sahashi, K. Inomata, *Adv. Cryog. Eng.* 32 (1986) 295.

Figure Captions

Fig. 1. Coordination polyhedra of the two crystallographically independent Gd sites in $\text{Gd}_4\text{Co}_2\text{Mg}_3$. Gd, Co and Mg atoms are drawn as medium gray, black

filled, and open circles, respectively. Atom designation and site symmetries are indicated.

Fig. 2. Temperature dependence of the reduced electrical resistivity of $\text{Gd}_4\text{Co}_2\text{Mg}_3$ between 4.2 and 280 K. The inset presents the T^2 dependence of the resistivity at low temperatures $T < 23$ K (the dashed line shows the linear dependence).

Fig. 3. Temperature dependence at various fields of the magnetization of $\text{Gd}_4\text{Co}_2\text{Mg}_3$ divided by magnetic field: (a) for $H = 0.025, 0.1$ and 0.2 T and (b) for $H = 0.85$ and 1 T. The inset of Fig. 3(a) presents the reciprocal magnetic susceptibility (measured at $H = 3$ T) *versus* temperature and the Curie-Weiss law (dashed line).

Fig. 4. Field dependence at various temperatures of the magnetization of $\text{Gd}_4\text{Co}_2\text{Mg}_3$: (a) for $H < 0.5$ T and (b) for $H < 4.6$ T.

Fig. 5. Field-temperature phase diagram of $\text{Gd}_4\text{Co}_2\text{Mg}_3$ deduced from the magnetization measurements.

Fig. 6. Temperature dependence without applied magnetic field of the specific heat $C_{p,0}$ of $\text{Gd}_4\text{Co}_2\text{Mg}_3$.

Fig. 7. Temperature and field dependences of the magnetic entropy change for $\text{Gd}_4\text{Co}_2\text{Mg}_3$ deduced from the magnetization measurements. $\Delta S_{M,F \rightarrow AF}^{PEAK}$ and $\Delta S_{M,P \rightarrow F}^{PEAK}$ denote the peak entropy changes, respectively, for the (F) to (AF) metamagnetic transition and for the (P) to (F) ordering transition.

Fig. 8. Normalized relative cooling power, $\text{RCP}/\Delta H$, plotted against the magnetic ordering temperature T_t for the $\text{Gd}_4\text{Co}_2\text{Mg}_3$ ternary compound (present work) and

the largest MCE materials [26-30].

Fig. 9. Normalized adiabatic temperature change, $RCP/\Delta H$, plotted against the magnetic ordering temperature T_t , for the best magnetic refrigerant materials in the range of 10-80 K [31-38].

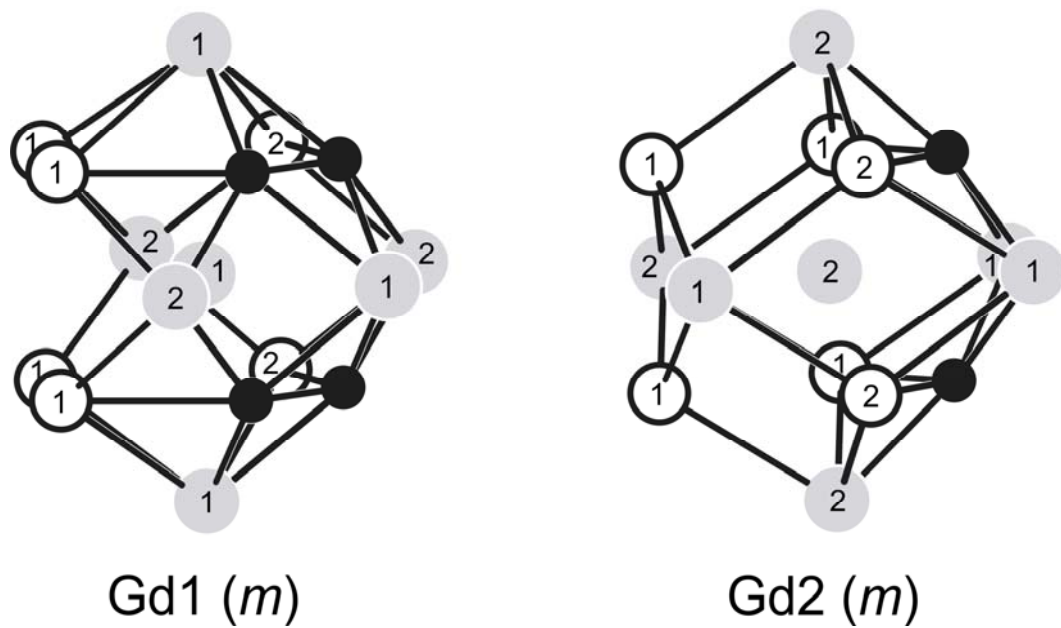


Fig. 1. Coordination polyhedra of the two crystallographically independent Gd sites in $Gd_4Co_2Mg_3$. Gd, Co and Mg atoms are drawn as medium gray, black filled, and open circles, respectively. Atom designation and site symmetries are indicated.

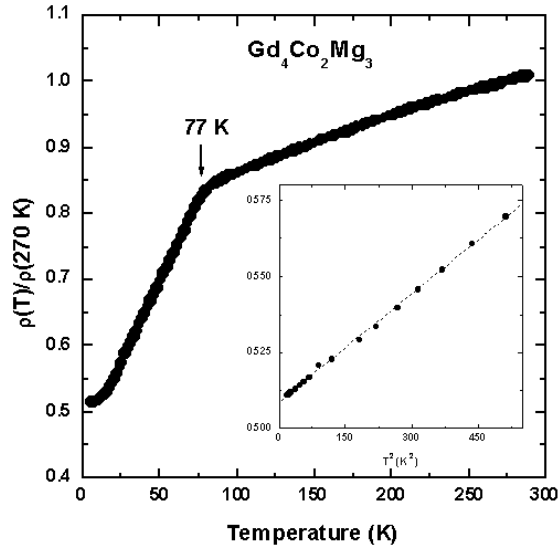


Fig. 2. Temperature dependence of the reduced electrical resistivity of $Gd_4Co_2Mg_3$ between 4.2 and 280 K. The inset presents the T^2 dependence of the resistivity at low temperatures $T < 23$ K (the dashed line shows the linear dependence).

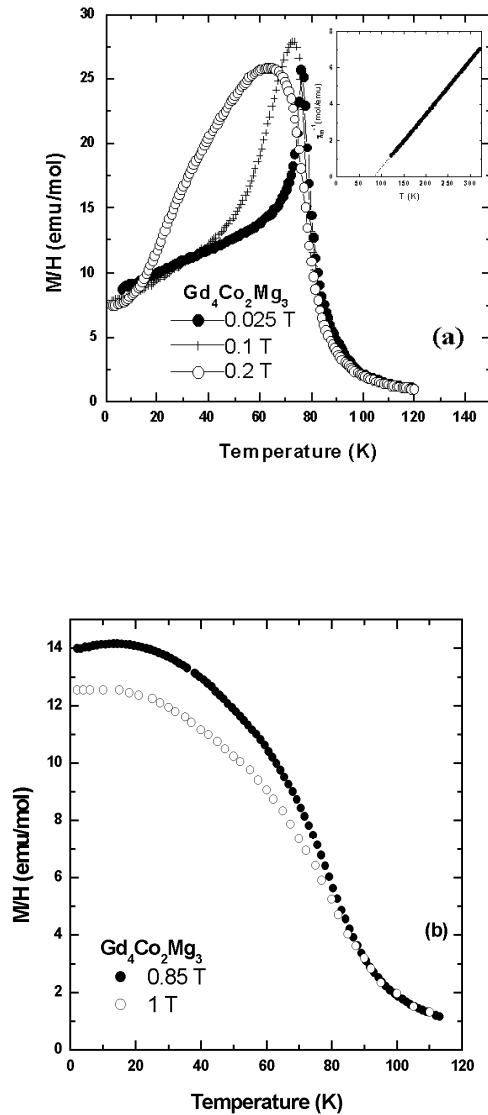


Fig. 3. Temperature dependence at various fields of the magnetization of $\text{Gd}_4\text{Co}_2\text{Mg}_3$ divided by magnetic field: (a) for $H = 0.025, 0.1$ and 0.2 T and (b) for $H = 0.85$ and 1 T. The inset of Fig. 3(a) presents the reciprocal magnetic susceptibility (measured at $H = 3$ T) *versus* temperature and the Curie-Weiss law (dashed line).

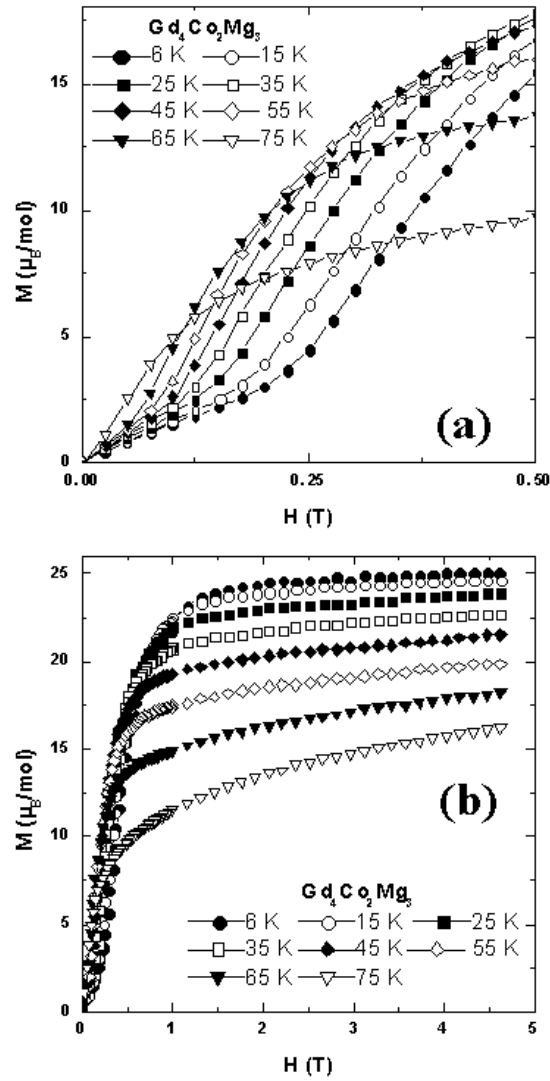


Fig. 4. Field dependence at various temperatures of the magnetization of $\text{Gd}_4\text{Co}_2\text{Mg}_3$: (a) for $H < 0.5$ T and (b) for $H < 4.6$ T.

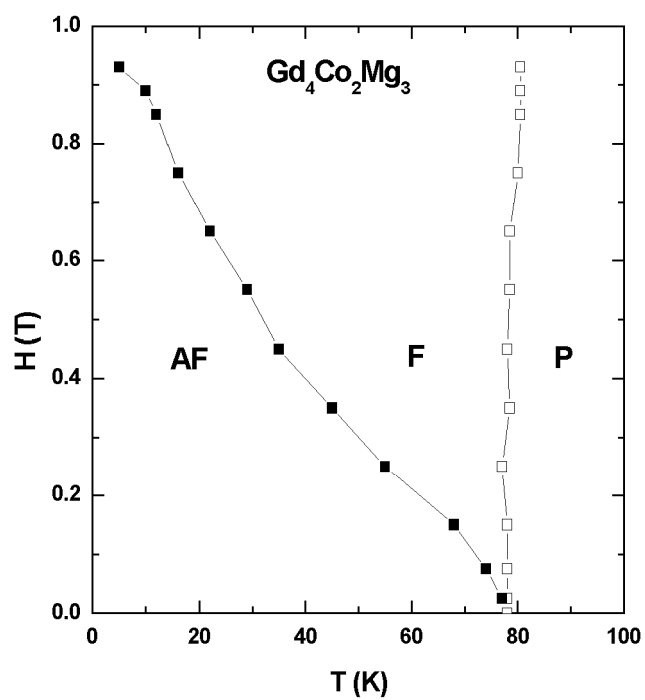


Fig. 5. Field-temperature phase diagram of $Gd_4Co_2Mg_3$ deduced from the magnetization measurements.

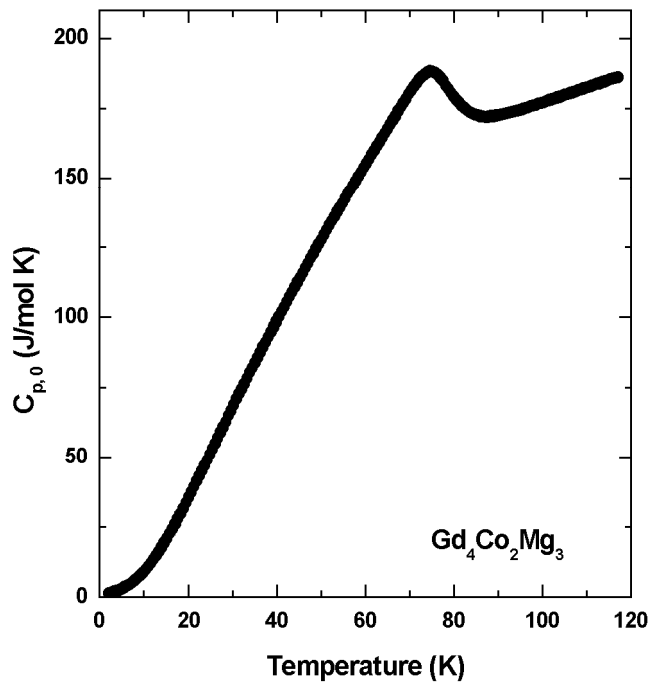


Fig. 6. Temperature dependence without applied magnetic field of the specific heat $C_{p,0}$ of $Gd_4Co_2Mg_3$.

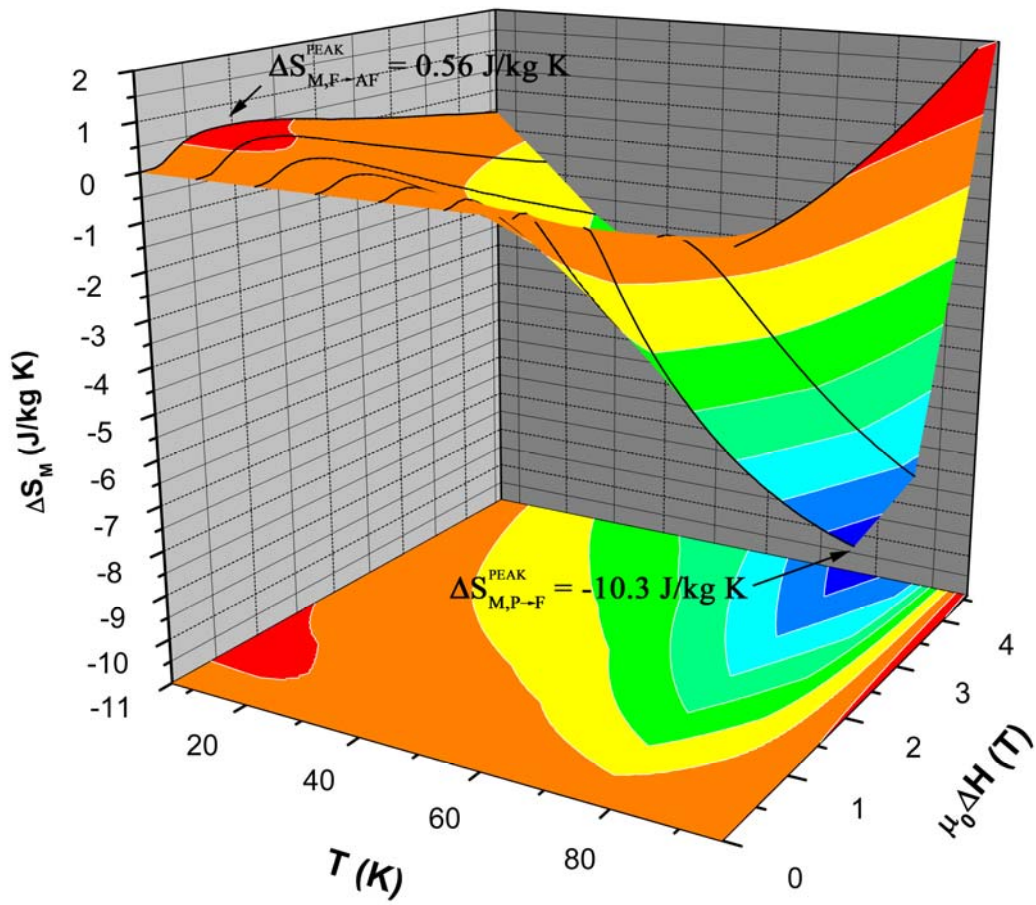


Fig. 7. Temperature and field dependences of the magnetic entropy change for $\text{Gd}_4\text{Co}_2\text{Mg}_3$ deduced from the magnetization measurements. $\Delta S_{M,F \rightarrow AF}^{PEAK}$ and $\Delta S_{M,P \rightarrow F}^{PEAK}$ denote the peak entropy changes, respectively, for the (F) to (AF) metamagnetic transition and for the (P) to (F) ordering transition.

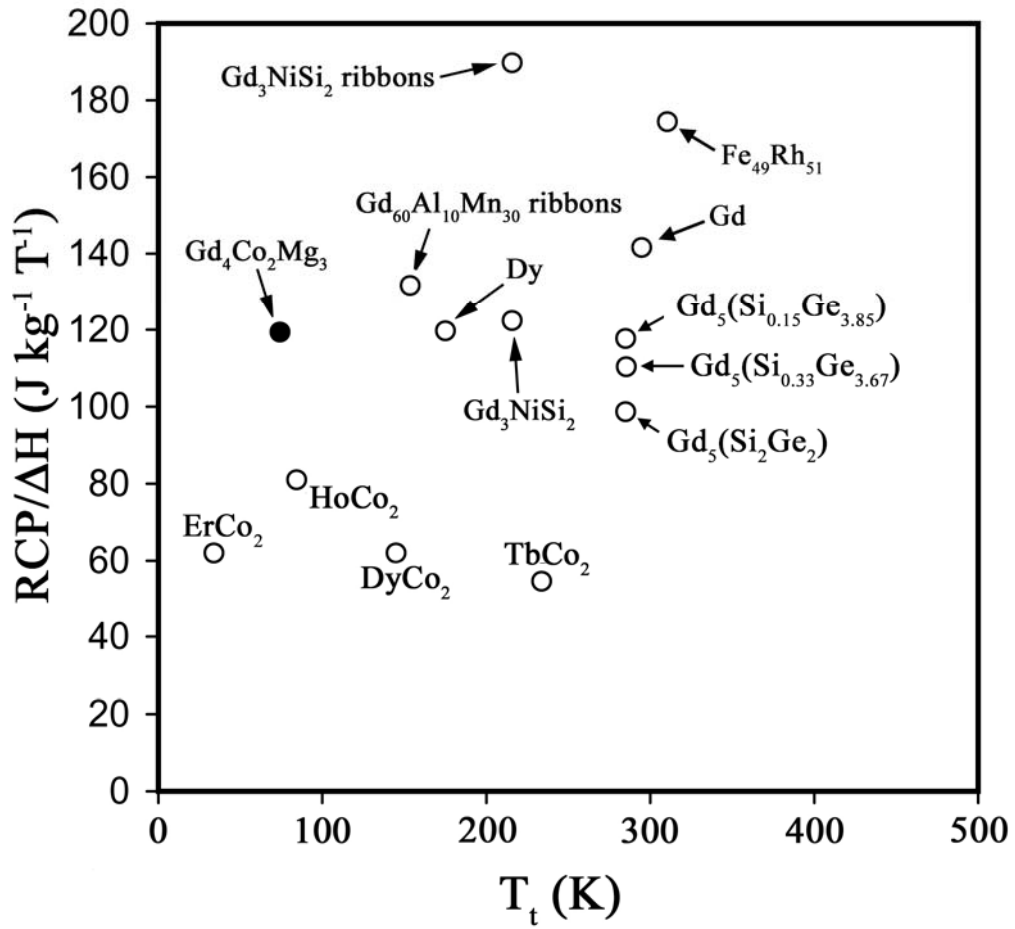


Fig. 8. Normalized relative cooling power, $RCP/\Delta H$, plotted against the magnetic ordering temperature T_t for the $Gd_4Co_2Mg_3$ ternary compound (present work) and the largest MCE materials [26-30].

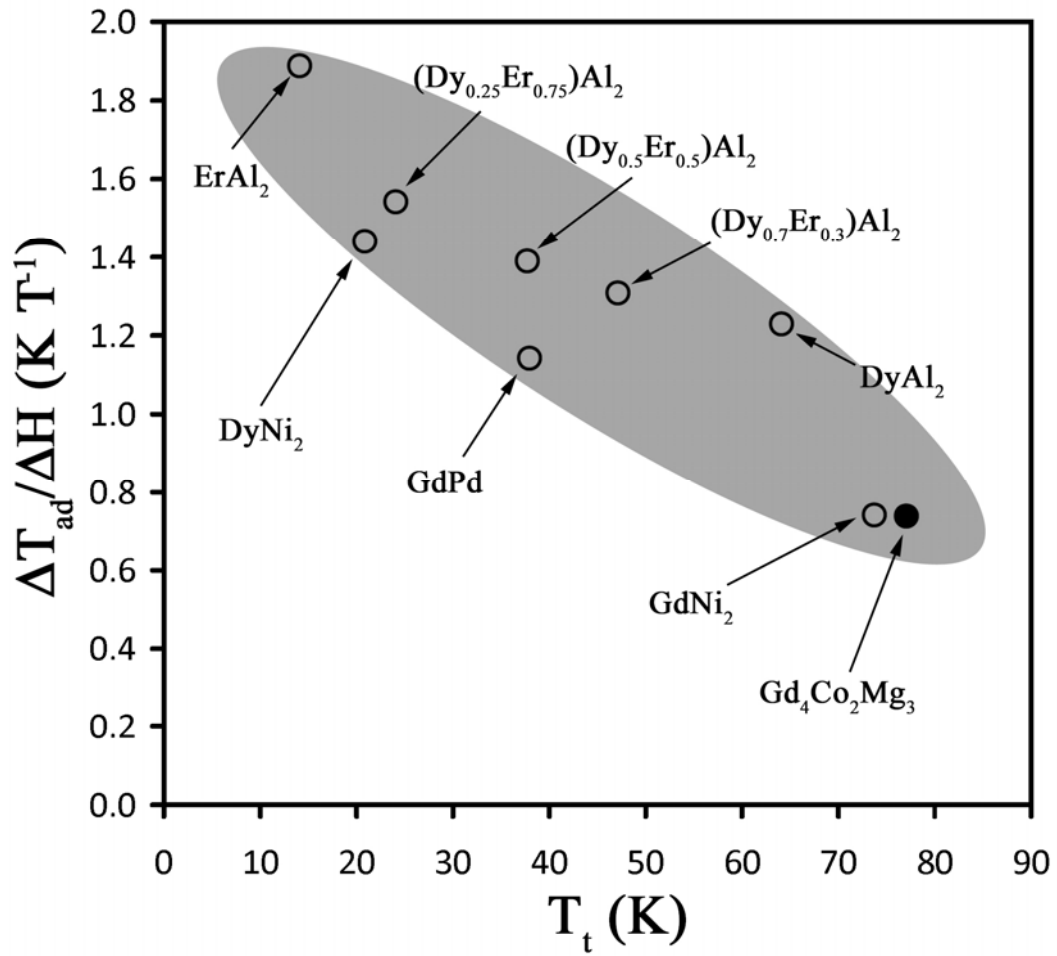


Fig. 9. Normalized adiabatic temperature change, $RCP/\Delta H$, plotted against the magnetic ordering temperature T_t , for the best magnetic refrigerant materials in the range of 10-80 K [31-38].